Experimental Mechanics (2007) 47:417–425
DOI 10.1007/s11340-007-9046-8

Flexible Probes for Characterizing Surface Topology: From Biology to Technology

A. Vaziri · R.A. Jenks · A.-R. Boloori · G.B. Stanley

Received: 20 December 2006 / Accepted: 27 February 2007 / Published online: 24 March 2007

Abstract In nature, several species use flexible probes to actively explore their environment and acquire important sensory information, such as surface topology, texture, and water or air flow velocity. For example, rats and other rodents have an array of facial vibrissae (or whiskers) with which they gather tactile information about the external world. The complex mechanisms by which mechanical deformations of the probe lead to neuronal activity in the animal's nervous system are still far from being completely understood. This is due to the intricacy of the deformation mechanics of the flexible sensors, the processes responsible for transforming the deformation to electrical activity, and the subsequent representation of the sensory information by the nervous system. Understanding how these mechano-sensory signals are transduced and extracted by the nervous system promises great insight into biological function, and has novel technological applications. To understand the mechanical aspect of sensory transduction, here we monitored the deformation of a rat's vibrissa as it strikes rigid objects with different topologies (surface features) during locomotion, using high-speed videography. Motivated by our observations, we developed detailed numerical models to study the mechanics of such flexible probes. Our findings elucidate how active sensation with vibrissae might provide sensory information and in addition have direct implications for several technological areas. To put this in perspective, we propose strategies in which flexible probes can be used to characterize surface topology at high speeds, which is a desirable feature in several technological applications such as memory retrieval.

Keywords Whisker mechanics · Flexible probes · Texture detection · Surface discrimination · Millipede technology

A. Vaziri (✉) · A.-R. Boloori · G.B. Stanley (✉)
School of Engineering and Applied Sciences,
Harvard University,
Cambridge, MA 02138, USA
e-mail: avaziri@seas.harvard.edu

G.B. Stanley
e-mail: gstanley@seas.harvard.edu

R.A. Jenks · G.B. Stanley
Department of Physics, Harvard University,
Cambridge, MA 02138, USA

Introduction

Measuring surface topology, from the nanometer to the kilometer scale, is a ubiquitous challenge in a number of scientific fields and technological applications. Examples range from the precise measurement of planetary geographical features to the characterization of sub-micron surface wrinkles in biological or industrial materials. Recent advances in the field of materials science have resulted in the ability to construct, and the need to characterize, features on the sub-micron scale [1–5]. These advances have far-ranging implications for an array of scientific and technological areas from tissue engineering to memory storage devices. In tissue engineering, for example, the surface topology alters how individual cells migrate, differentiate, interact with each other, and die [6–9]. Certain aspects of cell behavior can therefore be controlled by altering surface topology. For the development of memory devices, the ability to measure surface topology at high speeds and with high spatial resolution has provided new avenues for device development. For example, the 'Millipede' system allows surface features to be measured at a significantly higher spatial resolution than previous methods by employing hundreds of atomic force microscopy probes [10, 11].

Here, we focus on biologically inspired flexible probes for mapping of surface topology. Flexible probes are widely present in biological systems, and are utilized by several species as a robust tool to sense their environment [12–19]. For example, rodents have an array of flexible vibrissae (i.e. whiskers) on both sides of their face and can sense surface deformations on the micron scale by brushing the vibrissae against the surface. Due both to the animal's own behavior (body motion, head motion, vibrissa motion, etc.) and to an ever-changing external environment, there is significant variability in the physical manner in which object surfaces are probed. Despite this variability, the acquired information must somehow be optimally transmitted and invariantly linked to the absolute properties of the outside world. This is a critical problem for biological systems to solve, and the implementation of related biologically inspired strategies may also be highly advantageous for engineered devices which measure surface topology. However, flexible probes have not previously been thoroughly exploited in technological applications [20–22]. Here, we use the rat vibrissa as inspiration to study the mechanics of flexible probes and to examine the efficacy with which such probes can be used to measure the topology of a surface. We used high-speed videography to visualize the dynamics of a single vibrissa of an unrestrained rat as it contacted various surface features during locomotion. On the basis of these observations, we developed detailed numerical simulations using the finite element method (FEM) to gain insight into the mechanics of flexible probes (see the "Results and Discussions" Section). Finally, we highlight a potential technological application of flexible probes in the "Potential Technological Application of Flexible Probes" Section by focusing on their use in the reading stage of mechanical memory devices.

Materials and Methods

Visualization of Vibrissa Dynamics

One adult female Long-Evans rat was trained to run back and forth along a linear track. Animal maintenance and experimental procedures were conducted in accordance with the Animal Care and Use Committee of Harvard University and the guidelines established by the National Institutes of Health. All but one vibrissa on each side of the face were trimmed to facilitate imaging and to reduce the complexity of mechanical inter-vibrissa interaction. Tactile stimuli (surface features) were placed on either side of the track along a 10 cm length roughly equidistant from each end. Two tactile stimuli were considered to study the vibrissa dynamics: (1) A rigid object with a smooth surface made of clear acrylic, 10 cm long and 6 cm tall [Fig. 2(a)] and (2) a periodic 'surface' composed of vertically oriented stiff metal tubes (6 cm tall, 1 mm diameter) attached to acrylic mounts, spaced evenly apart with a spacing of 1 cm between the tubes [Fig. 4(a)].

Video was acquired using a high-speed CMOS camera (Phantom, Vision Research, Wayne, NJ). The camera was mounted directly above the region of interest defined by the tactile stimuli as shown in Fig. 1(a). Video was acquired at 2,000 frames per second and 950×512 pixels per frame, with a luminance resolution of 8 bits. Exposure time per frame was limited to 0.2 ms. The lens (Sigma, Tokyo, Japan, f=135 mm) was placed at a distance of 1 m from the track. This configuration allowed the entire 10×10 cm region of interest to be in focus, and resulted in a spatial resolution of 8.35 pixels per mm. The quality of the video was enhanced by backlighting the field. A custom-made 10×10 array of diode sub-arrays was utilized, where each sub-array consisted of a 2×4 pattern of red light-emitting diodes (Lumex, Platine, IL). A glass diffuser (ThorLabs, Newton, NJ) was placed 3 cm above the array and also formed the floor of the track in the region of interest. In each trial, the camera was triggered using an infra red beam which passed perpendicularly across the track just outside the textured region of interest.

Quantification of the Vibrissa Motion at the Base

In each trial, the rat's head and the vibrissa movement were tracked offline using a software package written by Knutsen and colleagues [23]. The software uses code written in MATLAB (v6.5, MathWorks, Natick, MA) and the C programming language. Head movements were tracked by following reflections of a halogen spotlight in two 4 mm diameter plastic beads glued to shaved areas behind the rat's eyes. Vibrissae were tracked in the head frame of reference using a 3-point spline-fitting algorithm (see [23] for details). The angular deflection of the vibrissa close to its base was estimated by calculating the angle of a straight line segment between the extreme points of a short (3 mm long) spline fitted to a segment of the vibrissa close to its base (within 2 mm of the mystacial pad). The computed signals were low-pass filtered with a cutoff frequency of 100 Hz to remove high-frequency image and tracking noise, which accounted for less than 0.1% of the power in the signal.

Numerical Simulation of the Flexible Probe Mechanics

To study the mechanics of flexible probes, a computational model was developed using commercially available finite element software (ABAQUS, Providence, RI) [24], as shown in Fig. 1(b). This computational model was employed to simulate the response of a flexible probe as

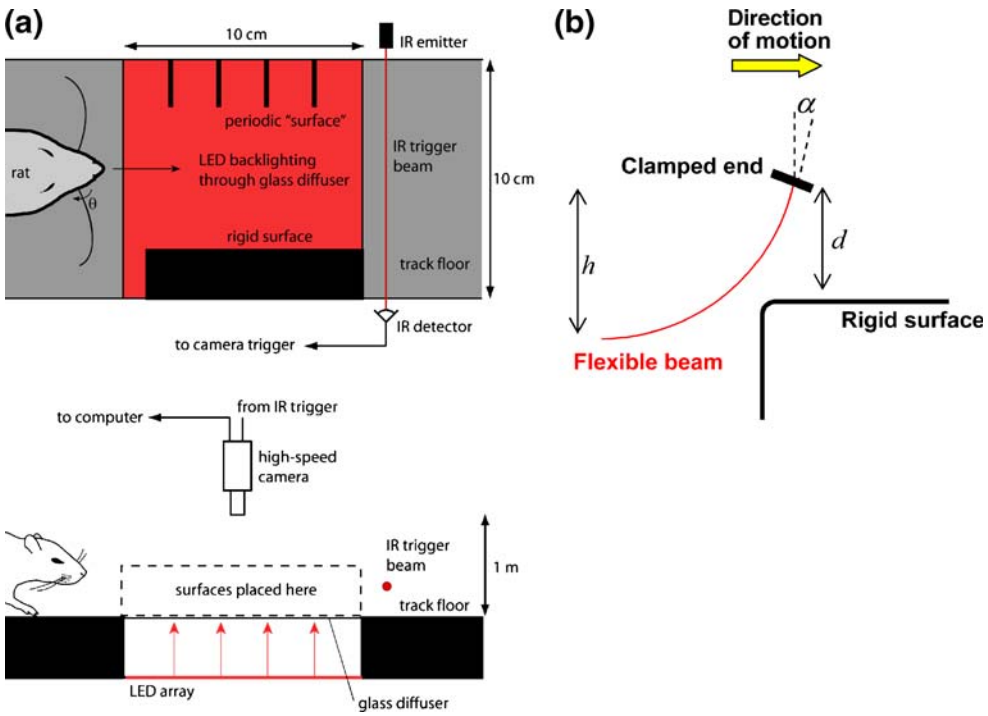

Fig. 1 Schematics of the experimental setup and computational model. (**a**) *Top*: Top view of track showing surfaces on either side, backlit image area, and IR trigger beam. Beam triggers camera to send buffered frames to computer after rat crosses image area. *Bottom*: Side view of track showing LED array and camera. (**b**) Schematic showing structure of the computational model and relevant parameters

it travels along a surface with varying topology. In all the calculations, the flexible probe was modeled as a linear elastic beam with Young's modulus of 7.8 GPa, a Poisson ratio of 0.3, a constant radius of 0.12 mm, and a length of 37 mm. These material constants were chosen based on the reported values for a typical rat vibrissa [25]. It should be noted that the rat vibrissa is actually tapered from the base to the tip. The set of computations carried out here does not incorporate this variation in the cross section of the beam. A limited set of calculations was carried out for tapered flexible probes, which, despite some quantitative differences with the model with constant cross-section, revealed similar qualitative behavior. A free slipping condition was assumed between the flexible probe and the surface. The surface was modeled as a rigid object in all the calculations, unless otherwise indicated. Furthermore, the flexible probe was taken to be clamped at its base with α=15° [Fig. 1(b)]. We did not explore the role that the boundary condition at the base of the probe plays in its deformation mechanics in detail, since the boundary condition defined by the mechanical interactions between the vibrissa and the tissue of the face is not well understood and varies significantly with the motor activity of the rat. We therefore utilized the boundary condition that would be most applicable in an artificial sensor. No attempt was made to vary the overall shape of the probe or α in this study. Data are presented in the form of dimensionless parameters. All the calculations were carried out in the quasi-static regime using Abaqus/Standard, which assumes inertial effects are negligible. Rats' vibrissae in contact with a surface have a relatively high damping characteristic, and the inertial effects on their deformation mechanics are negligible. This is confirmed by our high speed videography, which shows very little inertial dynamics. However, understanding the role of inertia is critical for developing high speed probes discussed in the "Potential Technological Application of Flexible Probes"-Section and is the focus of our future research.

Results and Discussions

The vibrissa, as a structural element, is a three-dimensional curved beam with varying cross-section. The boundary conditions at the base depend on the anatomical details of the hair follicle and surrounding tissue, some of which can in turn be controlled actively by the rat. Therefore, the deformation of the vibrissa as it strikes an object is governed by complicated mechanisms which themselves are functions of the animal's behavior. Figure 2(a) shows four single frames from a high-speed video, separated by 15 ms, as the rat runs down the track and a vibrissa strikes a smooth rigid object located at a normalized vertical base-to-surface distance of $d/h = 0.49$. By analyzing the high-speed videos using the method described in the "Quantification of the Vibrissa Motion at the Base" Section, we measured the variation of the angular deflection of the vibrissa close to its base as it deforms [Fig. 2(b)]. No attempt was made to convert this measurement into the moment applied at the base of the vibrissa, because of several key assumptions about the details of tissue structure and behavioral variables

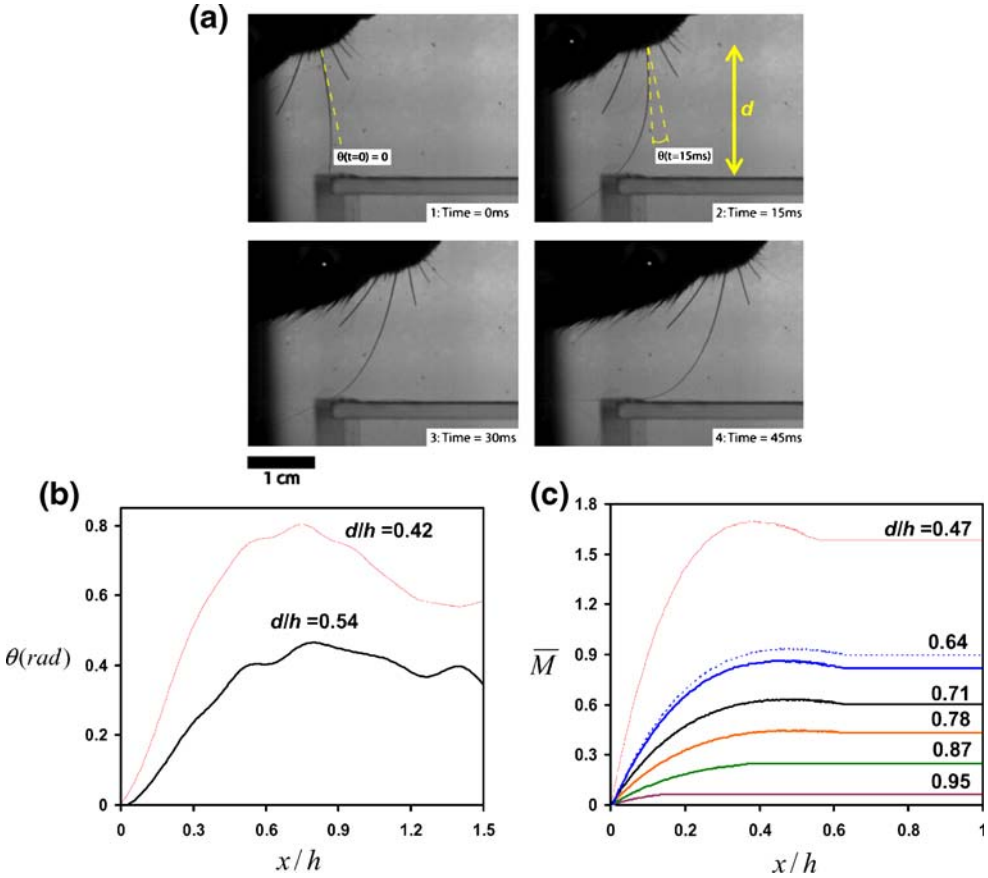

Fig. 2 Mechanics of vibrissa in contact with rigid objects. (**a**) Four frames of a high-speed video showing the sequence of the whisker deformation as the rat runs *from left to right* and whisker strikes a smooth rigid object located at a normalized vertical base-to-surface distance of $d/h = 0.49$. Whisker deformation is characterized using the angle measured in the head frame of reference, close to the base of the whisker. θ is defined as the difference between the measured angle and angle at t=0, as shown. (**b**) Measured angular displacement of whisker close to its base versus horizontal displacement of base for two values of d/h. The whisker makes contact with the object at x=0. (**c**) Variation of the normalized moment applied to the probe base (at its fixed end) versus x, for different vertical base-to-surface distances, d. In all the calculations, a free slipping condition was assumed for the contact, except one set of data for $d/h = 0.64$, where the coefficient of friction was taken as 0.5 (*dotted line*)

that would have to be made (see the "Numerical Simulation of the Flexible Probe Mechanics" Section). The results reveal the considerable sensitivity of the measured response to the vertical base-to-surface distance. In the plateau regime of the experimental measurements, the variation of the angular deflection is due to movement of the animal's head in the vertical direction (which can result from overall body motion, motion of the head relative to the body, or both). To complement these observations, numerical simulations using the flexible beam model described in the "Numerical Simulation of the Flexible Probe Mechanics" Section were carried out. In this set of calculations the distance between the base of the flexible probe and the surface that it strikes was varied systematically, while other parameters in the systems were kept constant. A selected set of numerical results is depicted in Fig. 2(c), where the variation of the moment applied to the base of the flexible probe is plotted versus the horizontal displacement of the base for different vertical base-to-surface distances. The calculated moment applied at the base of the probe is normalized by L/EI (L= 37 mm, I is the moment of inertia of the cross-sectional area of the beam with radius of 0.12 mm computed about its neutral axis, and E=7.8 GPa in all the calculations). This normalization constant is the theoretical approximation of the moment required for inducing one radian of rotation at the free end of a straight beam with the same material properties and length as the flexible probe subject to a constant moment, assuming infinitesimal deformation. The initial increase in the applied moment is followed by a plateau regime in the moment-displacement response. All of the computations in this study were carried out quasi-statically (i.e. without considering inertial effects).

Figure 3 shows the computed steady state normalized moment applied to the probe base, denoted by $\overline{M}_s$, as a function of the vertical base-to-surface distance. The experimental results obtained for a smaller range of d/h compared to the numerical simulations, are also shown in the same figure. The numerical simulations reveal the details of the nonlinear response of the flexible probe as it contacts objects located at different distances from its base. In the numerical simulations presented in Fig. 3, the coefficient of friction was taken to be zero, i.e. free sliding condition. Increasing the coefficient of friction leads to an increase in the moment applied to the probe base, as exemplified in Fig. 2(c) (dotted versus solid) for $d/h = 0.64$. It should be noted, however, that the frictional effects are relatively small (even for large friction coefficients), and thus the distance to the surface is well-predicted by the resultant moment. The findings of this study have direct implication for the development of sensory feedback for autonomous

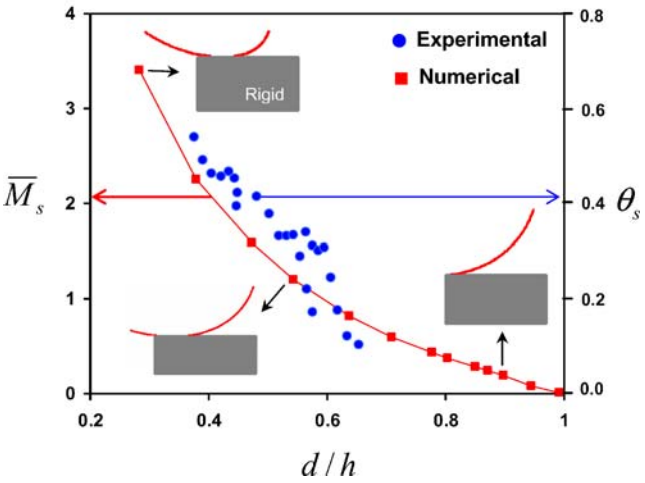

Fig. 3 Numerically simulated variation of the stationary normalized moment applied to the translating probe base while the probe is in contact with a rigid surface located at varying vertical base-to-surface distances, *d*. The experimental data are also superimposed on the same plot, showing the *d/h* dependence of the angular displacement of the whisker close to its base. Insets show the deformed configuration of the flexible probe for three different base-to-surface distances, *d*

robotic devices, in which it may be vital to utilize tactile sensors to determine proximity to external objects.

We also monitored the deformation of the vibrissa as it strikes a periodic surface created from a series of uniformly spaced rigid poles (period, denoted by λ), as shown in Fig. 4(a). The variation of the resultant angular deflection of the vibrissa close to its base versus the horizontal displacement of the head is shown in Fig. 4(b), for $\lambda/h = 0.36$. After the initial increase in the angular deflection as the vibrissa strikes the first pole, the angular deflection is periodic with a period equal to that of the surface. Note that in this configuration, the vibrissa is never out of contact with a pole, and never undergoes free vibration. The schematic of the corresponding numerical model is shown in Fig. 4(c). In all the calculations, the poles have a width of *w*, which was kept as constant and equal to 0.1 *h*, and have a half cylinder shape at the top with diameter equal to the width of the pole. The vertical base-to-surface distance, *d*, is defined here as the distance between the base of the probe and top point of the poles. The calculated snapshots of the flexible probe as it strikes the surface with $\lambda/h = 0.2$ are also superimposed in the same figure for different values of *x*. Figure 4(d) shows the numerically calculated variation of the moment at the base of the flexible probe, normalized again by *L/EI*, as the flexible probe strikes the surface comprised of the set of poles shown in Fig. 4(c). The response obtained from the numerical simulations is in qualitative agreement with the experimental observations, as shown in Fig. 4(b). This analysis suggests that the moment generated at the base of the vibrissa likely provides reliable, accurate information about the surface texture. This moment is transduced into neural signals by a variety of mechanoreceptors in the hair follicle for use by higher areas in the sensory pathway. The fact that texture information is accurately represented by a moment signal at the input to the neural system satisfies the minimal requirements for accurate encoding of texture information by the sensory system.

The results of several experimental trials in which the normalized base-to-surface distance ranged from 0.45 to 0.68 suggested that the amplitude of variation of the angular displacement, denoted by $\Delta\theta$ in Fig. 4(b), decreases with increasing *d/h*. We confirmed these observations by analyzing several more trials with $\lambda/h = 0.71$. To gain further insight into this relationship, a set of parametric studies was carried out by systematically varying *d/h* and *λ/h*. The results of this study are summarized in Figs. 5 and 6. The results quantify the dependence of $\Delta\overline{M}$, the amplitude of the moment variation as it strikes the surface, on wavelength λ [as defined in Fig. 4(d)] and on the geometrical parameters of the system mentioned above. The results presented in Fig. 5 again reveal the considerable sensitivity of the response to the base-to-surface distance, *d/h*. For each *d/h*, the dependence of $\Delta\overline{M}$ on *λ/h* is almost linear before approaching a critical point where the probe completely separates from one pole before fully contacting the next. In such a case, the probe undergoes free vibration after detaching from the first probe. Here, we limit our study to the regime in which full contact is always maintained and therefore free vibration never occurs. This situation is relevant in many biological and technological applications. In Fig. 5, this critical wavelength is denoted by the dashed lines and arrows for $d/h = 0.78$ and 0.95. For other values of *d/h* plotted in this figure, the critical period is larger than the range considered. For each *λ/h*, $\Delta\overline{M}$ is significantly less for $d/h = 0.64$ compared to the measured value of $\Delta\overline{M}$ for $d/h = 0.47$. Note that the calculated value of $\Delta\overline{M}$ for $d/h = 0.95$ in the range of surface periods depicted in Fig. 5 is comparable with the corresponding value associated with $d/h = 0.47$, implying that the value of *d/h* could not be unambiguously determined from $\Delta\overline{M}$ alone.

In Fig. 6, we constructed a map which shows the variation of $\Delta\overline{M}$ as a function of *d/h* and *λ/h*. The region denoted by *Dynamic events* (i.e. the probe detaches completely from one pole before fully contacting the next one) is shown in Fig. 6(a). When studying the mechanics of the flexible probes, as we approach the region corresponding to the dynamic events, the dependence of the amplitude of moment on the surface wavelength becomes nonlinear, as exemplified in Fig. 5. Full characterization of the response in this region requires extensive calculations, and was not the focus of the present study. Figure 6(b) shows the results for a selected range of *λ/h*, clearly indicating that for each surface detection task, the maxi-

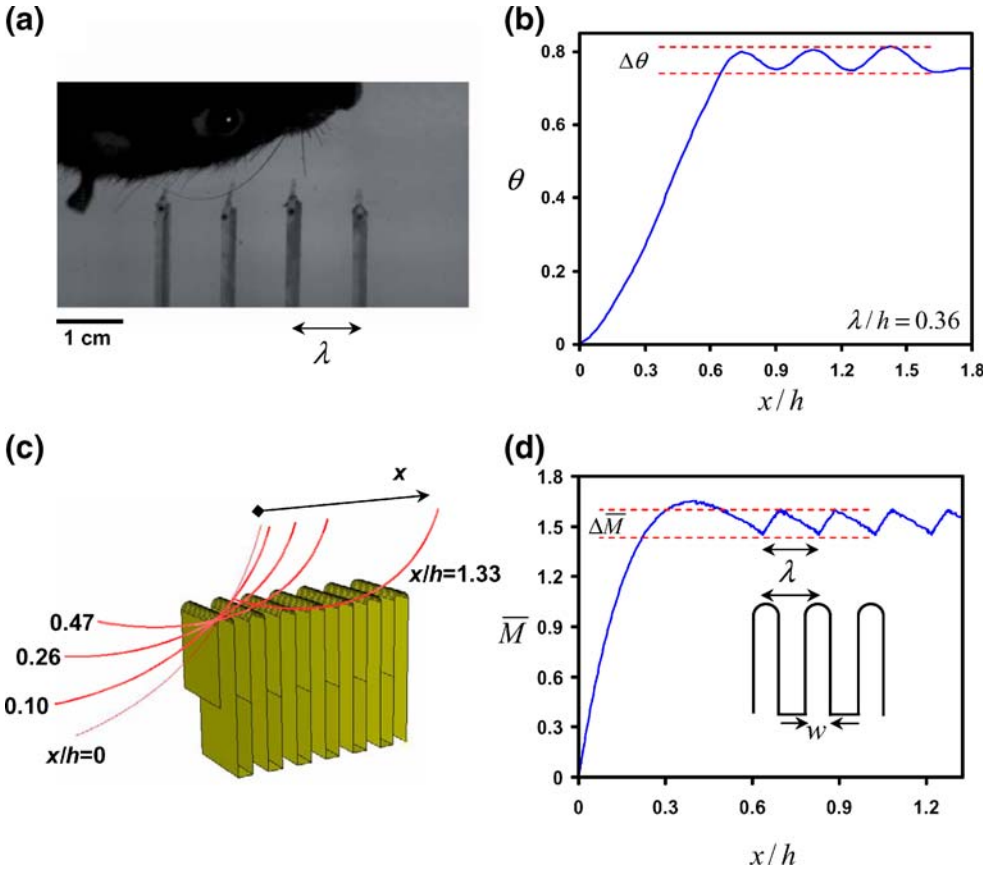

Fig. 4 Mechanics of vibrissa in contact with periodic surfaces. (**a**) Single high-speed video frame showing whisker deformation as rat runs from *left to right* and whisker strikes a surface with periodic features (poles), λ/h~0.36. (**b**) Angular deflection versus horizontal displacement. Here d/h~0.5. (**c**) Schematic of the computational model and the deformed configurations of the flexible probe at different stages of deformation. In this figure, $d/h = 0.47$. (**d**) Computed normalized moment, $\overline{M}$, versus horizontal displacement, showing similar trend as experimental measurements presented in (**b**). After the initial increase in moment, the response is periodic with period equal to that of the surface. Inset shows the configuration of the surface in the calculation. The width of each pole is denoted by w. The calculations are presented for $\lambda/h = 0.2$, $\lambda/w = 2$, and $d/h = 0.47$. Note that $\Delta\overline{M}$ is defined as the peak-to-peak amplitude of variations in $\overline{M}$

mum level of $\Delta\overline{M}$ is achieved at small and large values of d/h. The findings of this study have direct implications for devices developed to measure surface topology. Specifically, they suggest that probing surface features using a range of base-to-surface distances leads to a minimum value of the transmitted moment variation to the base and could lead to failure of the measurement task. An important parameter to consider is the ratio of the amplitude of the variation in the moment to the mean value of the moment. This ratio would be of considerable importance when developing devices, since small values of this ratio could be highly susceptible to measurement noise in the system. In Fig. 6(c), we have normalized the $\Delta\overline{M}$ by $\overline{M}_s$ for each d/h (see Fig. 3). This figure, which effectively displays the dependence of 'amplitude of variation in moment'/'mean moment applied to the probe base', suggests that higher values of d/h, approaching the total length of the probe, might lead to maximum sensitivity for characterizing the surface topology, while extra caution should be paid as dynamic effects could become important in this range.

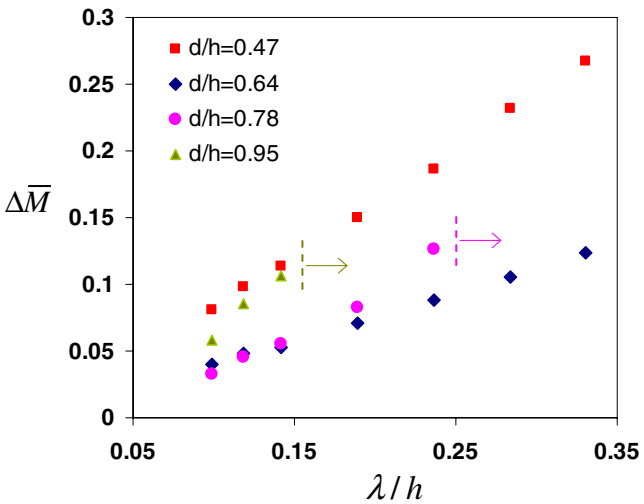

Fig. 5 Variation of $\Delta\overline{M}$ versus the normalized period of the surface features for various normalized vertical base-to-surface distances, d/h. The dotted lines and arrows show the limit above which dynamic effects become important, as the flexible probe fully detaches from one pole before achieving full contact with the next one. In this set of calculations, $w/h = 0.1$

Potential Technological Application of Flexible Probes

The detection of surface features has many technological applications, such as in reading systems for data storage devices, in characterizing the surfaces of semiconductor wafers and substrates, in MicroElectroMechanical systems (MEMS) and in mechanical biosensors. Here, we focus on

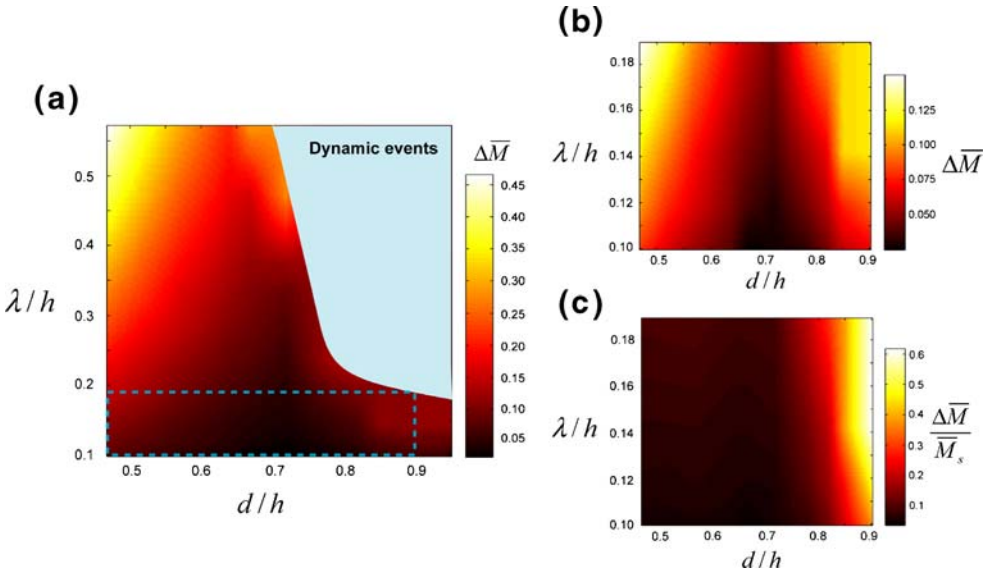

Fig. 6 (*color online*) Maps of the dependence of moment on geometric parameters. (**a**) Variation of $\Delta\overline{M}$ as a function of the normalized vertical base-to-surface distances, *d/h*, and the normalized period of the surface features, *λ/h*. The 'Dynamic events' region corresponds to the configurations in which the probe detaches completely from one pole before achieving full contact with the next one. It should be noted that as the combination of geometric parameters approaches the 'Dynamic events' limit, the accuracy of the moment calculation decreases. By reaching this limit, the response (i.e. dependence of $\Delta\overline{M}$ on the geometric parameters *d/h* and *λ/h*) becomes highly nonlinear as exemplified in Fig. 5. (**b**) Magnified region of (**a**) (*dashed rectangle*) with different moment scale to demonstrate variations in $\Delta\overline{M}$ with the geometric parameters. (**c**) Variation of $\Delta\overline{M}/\overline{M}_s$ as a function of the geometric parameters *d/h* and *λ/h*. To construct this figure, the values of $\Delta\overline{M}$ shown in (**b**) were normalized by the normalized moment applied to the base of the same flexible probe as it travels through a rigid surface located at vertical base-to-surface distances, *d/h* (quantified in Fig. 4). In this set of calculations, $w/h = 0.1$

the potential use of flexible probes in the reading stage of data storage devices. In mechanical memory devices, the 'writing stage' can be carried out using several methods, such as by the mechanical etching of bits onto the substrate using atomic force microscopy (AFM) [10, 26], or by the method invented by Vaziri et al. [31]—which is based on lateral perturbation of longitudinally-compressed shells. The capability of flexible probes for detecting these surface features at low speed is already demonstrated in the previous sections. However to maximize the efficiency of memory devices, it is desirable to detect these surface features at the highest possible speed. Here, we envision a system which consists of the following components [31]: (1) a mechanical flexible probe, which can be moved at controlled speeds over a surface, (2) a sensor connected to the base of this probe, and (3) an analysis system which utilizes a filtering algorithm to determine surface features of the substrate from the resulting vibrations of the flexible probe. The schematic of the proposed system is shown in Fig. 7. The probe can move at specified speeds along a desired trajectory. The vibration of the probe resulting from surface contact will be measured by a sensor (or multiple sensors) attached to the base of the probe. We currently envision that the following signals may be detected by the sensor(s): (1) torque/displacement at the probe base by using, for example, single-walled or multi-walled carbon

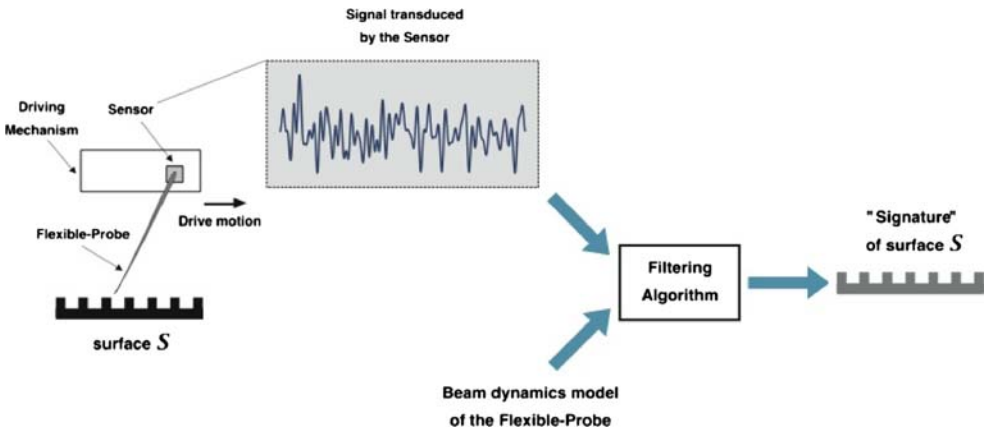

Fig. 7 The principle by which the proposed system senses textures. The proposed system consists of (1) a mechanical probe shaped as a flexible beam, which can be moved at controlled speeds over a surface, (2) a sensor connected to the base of the probe, and (3) an analysis system utilizing an algorithm to determine surface features from the resulting vibrations of the flexible probe. The result is a "signature" of the true surface topology

nanotubes [27–30] as torsional springs to signal submicron deformations or (2) the curvature of the sensor at each point, for example, by using fiber optic probes. Subsequently, the resulting signal(s) will be filtered to account for the dynamics of the probe. Ultimately, this filtering algorithm will yield a characteristic signature of the underlying surface, as schematically shown in Fig. 7. The filtering algorithm can be custom-made for a given surface detection task to minimize the time required for probing the surface topology. For example, if the surface is known to be periodic, then incorporating this knowledge into the filtering algorithm leads to simplification of the filtering step and may allow higher probing speeds.

In comparison to AFM probes, we envision that the proposed system will yield both higher spatial resolutions and higher probing speeds. The rigidity of the AFM beam limits the scanning speeds, especially for compliant substrates, and in cases when the substrate possesses sudden changes in surface topology. In these cases, the AFM tip can damage the substrate and its features. This limitation is overcome in the proposed method due to the flexibility of the probe. To gain the desired level of flexibility, for example, the probe can be made of polymer strands or sheets at the desired scale. Alternatively, stiffer materials, such as carbon nanotubes, can be used with more flexible interconnections. Several configurations are envisioned which can be employed based on the requirements of a given surface-detection task: possible configurations are a single discrete probe, multiple discrete probes, or a membrane-type probe. A single discrete probe allows for detection of the surface features along a desired line. Using multiple discrete probes allows detection of the surface features along multiple lines concurrently, as described before for the 'Millipede' system [10, 11] and arrays of polymeric nanomechanical biosensors [32, 33]. The continuum (membrane-type) flexible probe can ideally allow for detection of two-dimensional surface topologies with high spatial resolution. This system is currently in the early stages of development, and the validity of the claims regarding the superior performance of the proposed system in comparison to other commercially available systems is under study at this time.

Conclusions

Several species of animals utilize flexible probes to gather crucial sensory information about their natural environment, in many cases exhibiting surprisingly exquisite sensitivity in perceptual discrimination [19]. Despite their potential benefits, direct technological applications of such probes are still largely undeveloped. This study contributes to our knowledge of flexible probes in two important ways. Firstly, simultaneous use of empirical (high-speed videography) and finite-element studies illustrates and quantifies both the mechanics and the deformations of flexible probes as they strike surfaces with various topologies: upon repeated contact with periodic textures, both the mean value, and the amplitude of the moment transmitted to the probe's base are highly informative about the distance from the probe base to the surface. Additionally, the temporal variation of the moment unambiguously determines the spatial periodicity of the texture. Importantly, these observations illustrate that, by monitoring the time-history of the moment signal, an ideal-observer can infer the topology of the underlying surface at a length-scale that is significantly smaller than that of the probe. Of course, the quantitative features of all kinematic signals (e.g. angle, angular velocity, moment, etc.) transduced by the probe highly depend on both the probe-geometry, and surface-detail. Nevertheless, the above-mentioned findings are not case-dependent, and can be generalized to most probe-surface interactions.

Secondly, we have described the general features required of a device that can sense surface textures at higher speeds and spatial resolutions than are currently available. The range of potential applications for such a sensor is broad, including characterization of surface topology (similar to an AFM), reading of memory in data storage devices, etc. Further studies of animal behavior in acquiring and processing textural information may lead to additional important insights that may guide the sensor design and implementation. Active sensation involves a continuous interplay between the sensor and the surface, where the animal may modify behavior (e.g. body motion, head motion, angle, etc) and perhaps even sensor mechanics (e.g. boundary conditions) to optimize the information transmitted about the external environment. Such strategies, which have evolved under enormous evolutionary pressures over millions of years, may serve as a guiding design principle for the development of engineered devices for sensing surface topologies.

Acknowledgments AV would like to thank John W. Hutchinson for many insightful discussions. This work has been supported in part by The School of Engineering and Applied Sciences, Harvard University (AV) and in part by the Whitehall Foundation and the National Institutes of Health (NIH R01NS48285) (RAJ, AB, GBS).

References

1. Bowden N, Brittain S, Evans AG, Hutchinson JW, Whitesides GM (1998) Spontaneous formation of ordered structures in thin films of metals supported on an elastomeric polymer. Nature 393:146–149.
2. Kim KH, Moldovan N, Espinosa HD (2005) A nanofountain probe with sub-100 nm molecular writing resolution. Small 1:632–635.

3. Efimenko K, Rackaitis M, Manias E, Vaziri A, Mahadevan L, Genzer J (2005) Nested self-similar wrinkling patterns in skins. Nature Materials 4:293–297.
4. Espinosa HD, Zhu Y, Moldavan N (2007) MEMS based material testing systems: in-situ electron microscopy testing of nano objects. Encyclopedia of Materials: Science and Technology. Elsevier, in press.
5. Moon MW, Lee SH, Sun JY, Oh KH, Vaziri A, Hutchinson JW (2007) Wrinkled hard skins on polymers created by focused ion beam. Proc Natl Acad Sci U S A 104:1130–1133.
6. Chen CS, Mrksich M, Huang S, Whitesides GM, Ingber DE (1997) Geometric control of cell life and death. Science 276:1425–1428.
7. Jiang X, Takayama S, Qian X, Ostuni E, Wu H, Bowden N, LeDuc P, Ingber DE, Whitesides GM (2002) Controlling mammalian cell spreading and cytoskeletal arrangement with conveniently fabricated continuous wavy features on poly(dimethylsiloxane). Langmuir 18:3273–3280.
8. Jain R, von Recum AF (2003) Effect of titanium surface texture on the cell-biomaterial interface. J Invest Surg 16:263–273.
9. Lam MT, Sim S, Zhu X, Takayama S (2006) The effect of continuous wavy micropatterns on silicone substrates on the alignment of skeletal muscle myoblasts and myotubes. Biomaterials 27:4340–4347.
10. Vettiger P, Despont M, Drechsler U, Durig U, Haberle W, Lutwyche, MI, Rothuizen, HE, Stutz R, Widmer R, Binnig, GK (2000) The "Millipede"-more than one thousand tips for future AFM data storage. IBM J Res Develop 44:323–340.
11. Vettiger P, Cross G, Despont M, Drechsler U, Durig U, Gotsmann B, Haberle W, Lantz MA, Rothuizen HE, Stutz R, Binnig GK (2002) The 'millipede'-nanotechnology entering data storage. IEEE Trans Nanotechnol 1:39–55.
12. Camhi JM., Tom W, Volman S (1978) The escape behavior of the cockroach *Periplaneta americana*. II. Detection of natural predators by air displacement. J Comp Physiol 128:203–212.
13. Gnatzy W, Hustert R (1989) Mechanoreceptors in behavior. In: Huber F, Moore TE, Loher W (eds) Cricket behavior and neurobiology. Cornel University Press, Ithaca, NY, pp 198–226.
14. Welker WI (1964) Analysis of sniffing of the albino rat. Behaviour 12:223–244.
15. Wineski LE (1983) Movements of the cranial vibrissae in the golden hamster (*Mesocritus aurutus*). J Zool Lond 200:261–280.
16. Wineski LE (1985) Facial morphology and vibrissal movement in the golden hamster. J Morphol 183:199–217.
17. Arabzadeh E, Zorzin E, Diamond ME (2005) Neuronal encoding of texture in the whisker sensory pathway. PLOS Biol 3(1):e17.
18. Hipp J, Arabzadeh E, Zorzin E, Conradt J, Kayser C, Diamond ME, Konig P (2006) Texture signals in whisker vibration. J Neurophysiol 95:1792–1799.
19. Carvell GE, Simons DJ (1990) Biometric analyses of vibrissal tactile discrimination in the rat. J Neurosci 10:2838–2848.
20. Solomon JH, Hartmann MJ (2006) Biomechanics: robotic whiskers used to sense features. Nature 443:52.
21. Schultz AE, Solomon JH, Peshkin MA, Hartmann MJ (2005) Multifunctional whisker arrays for distance detection, terrain mapping, and object feature extraction. Proceedings of the 2005 IEEE International Conference on Robotic and Automation, pp 2588–2593.
22. Fend M (2005) Whisker-based texture discrimination on a mobile robot. In advances in artificial life. Springer, Berlin Heidelberg New York.
23. Knutsen PM, Derdikman D, Ahissar E (2005) Tracking whisker and head movements in unrestrained behaving rodents. J Neurophysiol 93:2294–2301.
24. ABAQUS/Explicit User's Manual (2001) Version 6.0. Hibbit, Karlsson and Sorensen Inc.
25. Neimark MA, Andermann ML, Hopfield, JJ, Moore, CI (2003) Vibrissa resonance as a transduction mechanism for tactile encoding. J Neurosci 23:6499–6509.
26. King WP, Kenny TW, Goodson KE, Cross G, Despont M, Durig U, Rothuizen H, Binnig GK (2001) Atomic force microscope cantilevers for combined thermomechanical data writing and reading. Appl Phys Lett 78:1300–1302.
27. Williams PA, Papadakis SJ, Patel AM, Falvo MR, Washburn S, Superfine R (2002) Torsional response and stiffening of individual multiwalled carbon nanotubes. Phys Rev Lett 89:255502.
28. Papadakis SJ, Hall AR, Williams PA, Vicci L, Falvo MR, Superfine R, Washburn S (2004) Resonant oscillators with carbon-nanotube torsion springs. Phys Rev Lett 93:146101.
29. Meyer JC, Paillet M, Roth S (2005) Single-molecule torsional pendulum. Science 309:1539–1541.
30. Hall AR, An L, Liu J, Vicci L, Falvo MR, Superfine R, Washburn S (2006) Experimental measurement of single-wall carbon nanotube torsional properties. Phys Rev Lett 96:256102.
31. Vaziri A, Boloori A-R, Stanley GB (2007) Flexible probes for detection of surface features. Patent Pending, USA.
32. Calleja M, Tamayo J, Johansson A, Rasmussen P, Lechuga L, Boisen A (2004) Polymeric cantilever arrays for biosensing applications. Sensor Lett 1:1–5.
33. Calleja M, Tamayo J, Nordström M, Boisen A (2006) Low-noise polymeric nanomechanical biosensors. Appl Phys Lett 88:113901.